International Journal of Environmental Science and Technology (2023) 20:5169–5182
https://doi.org/10.1007/s13762-022-04325-2

ORIGINAL PAPER

Electrochemical degradation of aqueous metformin at boron-doped diamond electrode: kinetic study and phytotoxicity tests

R. Chaabene[1] · L. Khannous[1] · Y. Samet[1]

Received: 13 October 2021 / Revised: 8 February 2022 / Accepted: 26 May 2022 / Published online: 27 June 2022

Abstract
The present study explores the galvanostatic electrolysis of synthetic solutions containing the antidiabetic metformin with different support electrolytes, using a boron-doped diamond anode in an undivided electrochemical cell to test the possibility of the reuse of the treated water in the field of agriculture. It also investigated the effects of the main operating parameters, including applied current density, supporting electrolyte nature and concentration, initial chemical oxygen demand, initial pH, temperature, and NaCl concentration. This was realized considering the chemical oxygen demand removal, current efficiency, energy consumption and phytotoxicity. The experimental results showed that metformin concentration, measured by the square wave voltammetry technique and the chemical oxygen demand decay, follows a pseudo-first-order kinetics. At the beginning of the electrolysis, the electrochemical efficiency was limited by a charge-transfer process. For an initial chemical oxygen demand of 900 mg L^{-1} and under optimal conditions (current density of 30 mA cm^{-2}, pH 2, Na_2SO_4 2 g L^{-1}, NaCl 0.8 g L^{-1} and T 343.15 K), the removal of organic matter was about 90% and the complete elimination of metformin was reached after 2 h of electrolysis. Concerning the phytotoxicity tests of the treated water, they were carried out using Fenugreek and Lucerne seeds. The results indicated a positive effect on seeds germination due to the production of nitrate ions from the metformin molecules.

Keywords Electrolysis · Irrigation · Pharmaceutical products · Reuse · Treatment

Introduction

The residues of pharmaceuticals as an emerging contaminant have become a major concern because of their prevalence and persistent accumulation in various environmental compartments. Therefore, their elimination has become an urgent necessity (Papageorgiou et al. 2019; Escudero et al. 2020; García et al. 2020; Kairigo et al. 2020).

Among the most extensively used pharmaceuticals, antidiabetic drugs can be foregrounded. According to the World Health Organization, around 422 million adults (Over 18 years) were living with diabetes in 2014 (WHO 2016), and in 2019, the number increased to 463 million adults (20–79 years) (IDF Diabetes Atlas 2019). The number of people with type-2 diabetes is increasing in most countries; approximately 87–91% of all people with diabetes suffer from type-2 diabetes (Cho et al. 2018).

Metformin hydrochloride (MTF) with the chemical name 1,1-dimethyl biguanide hydrochloride ($C_4H_{11}N_5$.HCl) is considered as the most utilized pharmaceutical for the treatment of type 2-diabetes (Sanchez-Rangel and Inzucchi 2017). MTF has an anticancer (Mallik and Chowdhury 2018), antiobesity (Malin and Kashyap 2014), antimicrobial (Patil et al. 2018) and antitumor activity (Zhang et al. 2020). It has also been associated with regulating the menstrual cycle and most hormonal profiles of women with polycystic ovary syndrome (Yang et al. 2018). Therefore, the extensive use of MTF can cause the contamination of aquatic medium and water sources. In wastewater treatment plants (WWTPs) effluent, the concentrations of MTF range from 2.42 to 248 µg L^{-1} (Ottmar et al. 2010; Tong et al. 2015; Briones et al. 2016; Yan et al. 2019). Only 10% of MTF can be absorbed in the human body and the rest is excreted unchanged in the urine and feces and posed an

Editorial responsibility: Samareh Mirkia.

✉ R. Chaabene
chaabene.rania92@gmail.com

[1] Laboratoire de Toxicologie Microbiologie Environnementale et Santé (LR17ES06), Sciences Faculty of Sfax, University of Sfax, B.P. 1173, 3038 Sfax, Tunisia

environmental concern (Dolatabadi and Ahmadzadeh 2019). MTF is biologically transformed into guanylurea as a major degradation product (Scheurer et al. 2012).

Three further transformation products, namely 2,4-diamino-1,3,5-triazine (2,4-DAT), 2-amino-4-methylamino-1,3,5-triazine (2,4-AMT) and methylbiguanide (MBG), have been detected in WWTPs effluents and surface waters (Elizalde-Velázquez and Gómez-Oliván 2020). Recently, (Gabr et al. 2017) have studied the pharmacokinetics of metformin and guanylurea in rats and indicated that approximately 92–100% of the molecules absorbed by the rat are released from the body after use. MTF and its transformation products accumulate in edible plant species (plant tissue) (Eggen and Lillo 2012), fish (Niemuth et al. 2015) and mussels (Koagouw and Ciocan 2018). Therefore, MTF and its metabolites not only pose a threat to humans, plants and the aquatic environment, also they are considered endocrine disruptors (Lee et al. 2019). For this reason, it is very important to develop technologies for the removal of these pharmaceutical products able to reduce the impact of these compounds on the environment.

Conventional wastewater treatment methods such as MTF adsorption (Zhu et al. 2017; Alnajjar et al. 2019; Adel Niaei and Rostamizadeh 2020; Balasubramani et al. 2020) and biodegradation have shown to be ineffective, with numerous environmental problems (Trautwein and Kümmerer 2011).

Thus, a growing interest has been shown in the use of new methods, namely advanced oxidation process (AOPs), which involves the generation of strong oxidants in situ, as an attractive solution used in the treatment of pharmaceutical products in water.

Various AOPs have been used for the degradation of MTF, among which the photo-Fenton process (De la Cruz et al. 2013). The best results of MTF were obtained when using UV (254 nm)/H_2O_2(30 mg L^{-1})/Fe^{2+}(2 mg L^{-1}) at pH between 6 and 7. After 30 min of treatment, the removal of MTF reached 63%. Recently, (Chinnaiyan et al. 2019) have studied the heterogeneous photocatalytic process using UV light at 365 nm and TiO_2 as photocatalyst at different dosages. Indeed, the maximum removal of MTF (98%) has been obtained when TiO_2 dosage is 563 mg L^{-1}, pH is 7.6 and a reaction time of 150 min for an initial concentration of the drug of 10 mg L^{-1}. (Carbuloni et al. 2020) have investigated the photodegradation of MTF at 298.15 K for catalysts TiO_2 and TiO_2–ZrO_2 (95–5) at pH 8 and found that the degradation of MTF followed a pseudo-first-order kinetics with MBG intermediate as a major identified by-product. The best eliminatory conditions (55%) were obtained after 30 min of treatment and proved to be a pH of 8 and 1 g L^{-1} for the two catalysts. This shows that the addition of ZrO_2 did not provide any improvement in the activity of the TiO_2 photocatalyst. Besides, (Orata et al. 2019) have investigated the degradation of MTF by an electro-Fenton process using boron-doped diamond (BDD) ($20 \times 50 \times 1$ mm^3) as anode and carbon felt ($30 \times 60 \times 5$ mm^3) as a cathode. The authors have found that the electrolysis of 0.2 mmol L^{-1} MTF under optimal conditions (0.3 mmol L^{-1} Fe^{2+}; an applied current of 300 mA and pH 3) leads to 99.57% of MTF removal after 27 min of electrolysis.

Electrochemical oxidation process under potentiostatic mode has also been explored with a BDD anode in the study of (Tisler and Zwiener 2018), in which the electrode was subjected to a potential of 1.5 V vs Ag/AgCl for 10 min in a two-compartment cell at pH 3 and 7. This research aims to study the presence and fate of MTF and its by-products in wastewater and surface water. Although the degradation products, namely 2,4-DAT, 2,4-AMT, MBG and 4-amino-2-imino-1-methyl-1,2-dihydro-1,3,5-triazine (4,2,1-AIMT), were identified, the well-known oxidation product guanylurea was not formed electrochemically. This observation could be due to the low value of the potential (1.5 V vs Ag/AgCl) applied to the BDD electrode. On the other hand, (Lović et al. 2019) have studied the direct electrochemical oxidation of MTF using Au, glassy carbon and IrOx electrodes and Na_2SO_4 as electrolyte. The highest total organic carbon reduction of 10.6% was obtained with the IrOx electrode. This study has demonstrated that the electrode materials used are not suitable for a better degradation of MTF and its by-products.

The present study aims to achieve the complete degradation of MTF and its reaction intermediates by electrochemical oxidation under galvanostatic mode using a BDD anode. The optimization of key experimental parameters, such as the applied current density, the nature of the supporting electrolyte, the initial chemical oxygen demand, the temperature, and the addition of NaCl, was conducted, and the treatment efficiency was examined by phytotoxicity tests via the germination of Fenugreek (Trigonella foenum-graecum) and Lucerne (Medicago sativa) seeds. The time span of this research study was from October 2020 to July 2021 at the Faculty of Sciences of Sfax, Tunisia.

Materials and methods

Chemicals

Metformin hydrochloride (97%), sulfuric acid (95%), sodium hydroxide (97%), potassium dichromate (99%), silver sulfate (99.5) and mercury sulfate (96%) of analytical grade were purchased from Sigma-Aldrich. Na_2SO_4 (99.5%) was obtained from Prolabo (Paris-France). All solutions were freshly prepared with double-distilled water.

Electrolysis cell

The galvanostatic electrolyses of MTF solutions (200 mL) were carried out in a one-compartment thermostatted glass cell (300 mL). A boron-doped diamond (BDD) electrode with a geometric area of 6 cm^2 was provided by CSEM (Centre Suisse d'Electronique et de Microtechnique, Neuchâtel, Switzerland). It was synthesized by the hot filament chemical vapor deposition technique (HF-CVD) on single-crystal p-type Si < 100 > wafers (1–3 mΩ cm, Siltronix) (Perret et al. 1999). The doping level of boron in the diamond layer expressed as B/C ratio was about 3500 ppm using trimethyl boron with a concentration of 3 ppm. The obtained diamond film thickness was about 1 µm with a resistivity of 10–30 mΩ cm. Before each electrolysis assay, the BDD electrode was subjected to an anodic polarization in 0.5 mol L^{-1} H_2SO_4 solution at a constant anodic current density of 50 mA cm^{-2} for 30 min to regenerate its surface. A stainless-steel plate (10 cm^2 in contact with the solution) in the electrolyte delivery system acts as the cathode. The MTF solutions were electrolyzed in galvanostatic mode with current densities in the range of 5–40 mA cm^{-2} using a Laboratory DC Power Supply GW Dual Tracking Power Supply 5 V Fixed Model: GPC-3030. The electrolyte is stirred through a magnetic bar at a constant speed. The pH of the solution was adjusted, before and throughout the electrolysis, by adding either sulfuric acid or sodium hydroxide solutions (1 mol L^{-1}).

Chemical oxygen demand, current efficiency, limiting current and specific energy consumption

The degradation process of the organic matter was evaluated by the measurement of the chemical oxygen demand (COD). The COD was estimated by the conventional method with $K_2Cr_2O_7$ as the oxidizing agent (Hejzlar and Kopáček 1990). The appropriate amount of the sample was introduced into a prepared digestion solution containing potassium dichromate, sulfuric acid and mercury (II) sulfate. Afterward, the mixture was incubated for 2 h at 423.15 K in a DRB 200 HACH thermo-reactor. The values of COD were measured colorimetrically with a JENWAY 6305 spectrophotometer.

The COD removal rate (%) was calculated using Eq. (1)

$$\text{COD removal}(\%) = \frac{\text{COD}_0 - \text{COD}_t}{\text{COD}_0} \times 100 \quad (1)$$

where COD_0 and COD_t (g O_2 L^{-1}) are the chemical oxygen demands at times $t = 0$ and t, respectively.

The current efficiency (CE) for the anodic oxidation of MTF was calculated from the values of the COD according to Eq. (2).

$$\text{CE}(\%) = \frac{\text{COD}_0 - \text{COD}_t}{8It} FV \times 100 \quad (2)$$

where I is the current (A), F is the Faraday constant (96,485 C mol^{-1}), V is the volume of the solution (L), 8 is the oxygen equivalent mass (g $equiv^{-1}$) and t is the electrolysis time (s).

In electrochemical processes, according to the value of current density, two different kinetic regimes for a given reactant concentration can be defined (Rodrigo et al. 2001).

According to applied (j_{app}) and limiting (j_{lim0}) current densities values:

- If $j_{app} < j_{lim0}$, the electrolysis is under charge transfer control, CE (%) is then 100%.
- If $j_{app} > j_{lim0}$, the electrolysis is under mass transport control, secondary reactions (such as oxygen evolution) occur.

Additionally, (j_{limt}) was estimated using Eq. (3) which is associated with the electrochemical combustion of the MTF [Eq. (4)]:

$$j_{limt} = 52Fk_m c_t \quad (3)$$

$$C_4H_{12}N_5Cl + 23\ H_2O \rightarrow 4\ CO_2 + 5\ NO_3^- + 58\ H^+ + 52\ e^- + Cl^- \quad (4)$$

where k_m is the average mass transport coefficient and c_t is the MTF concentration (mol m^{-3}) at a given time t.

The stoichiometry of MTF combustion indicates that 13 mol of O_2 are needed for its complete combustion [Eq. (5)]

$$C_4H_{12}N_5Cl + 13\ O_2 \rightarrow 4\ CO_2 + 5\ NO_3^- + 6\ H^+ + 3\ H_2O + Cl^- \quad (5)$$

Thus, during the electrolytic process, the MTF concentration c_t (mol m^{-3}) is related to the COD_t (mol m^{-3}) by Eq. (6):

$$\text{COD}_t = 13\ c_t \quad (6)$$

Accordingly, j_{limt} can be written as a function of COD_t by Eq. (7):

$$j_{limt} = \frac{52}{13} Fk_m \text{COD}_t = 4Fk_m \text{COD}_t \quad (7)$$

The specific energy consumption (Ec) (kWh m^{-3}) calculated by Eq. (8) is an essential parameter for evaluating the efficiency of the electrochemical process.

$$\text{Ec} = \frac{U_{cell} It}{3600V} \quad (8)$$

where U_{cell} is the average cell voltage (V), I is the applied current (A), t is the electrolysis time (s) and V is the volume of the treated solution (L).

Square wave voltammetry

The decrease in MTF concentration was carried out by square wave voltammetry (SWV) analysis in three-electrode cell experiments using a potentiostat–galvanostat (VoltaLab PST050) at 293.15 K.

The working electrode was a BDD disc with a geometrical surface of 0.07 cm^2. A stainless steel plate (0.1 cm^2) and a saturated calomel electrode (SCE) were used as the auxiliary electrode and the reference electrode, respectively.

Before each experiment, the BDD anode was exposed to potential cycling conditions in sulfuric acid (0.5 mol L^{-1}) between −3.0 and 3.0 V at a scan rate of 5 V s^{-1} for 120 s, and then, it was rinsed with bidistilled water. The samples of 1 mL were taken at different electrolysis times and diluted 10 times with bidistilled water containing 2 g L^{-1} Na_2SO_4. The pH was adjusted at 12.5 using 1 mol L^{-1} NaOH solution in order to obtain a well-defined anodic peak.

Ion chromatography (IC) analysis

The concentration of NH_4^+ produced during treatment was measured by the standard colorimetric technique using Nessler's reagent and a Unicam UV–vis UV4 spectrophotometer thermostated at 298 K. In the same samples, NO_3^- concentration was determined by ion chromatography using a Shimadzu 10AVP HPLC system fitted with a Shim-pack IC-A1 anion column ((4.6 mm (I.D.) × 100 mm (Length)) at 313 K coupled with a Shimadzu CDD-10AVP conductivity detector.

Germination test

Phytotoxicity tests were conducted to assess the possibility of the reuse of the treated water in irrigation fields. Two plants (Fenugreek and Lucerne seeds) were chosen for the irrigation tests with different water samples.

The seeds of Fenugreek and Lucerne were sterilized with 20 mL of sodium hypochlorite solution (20%) for 10 min and then abundantly rinsed with sterilized distilled water. The seeds of uniform size were placed on filter paper in circular dishes of Petri with a diameter of 90 mm and then irrigated with 10 mL of the different treated water samples. The tests were conducted in duplicates. The seeds were germinated in the dark for two days and in the light for eight days at room temperature. For comparison, tap water and distilled water were tested instead of the present treated water. These experiments were repeated three times. The study of plant modification morphology assessed the impact of water quality on plant growth and the germination index (GI) was calculated according to the following equation (Zayneb et al. 2015):

$$\mathrm{GI}(\%) = \left(\frac{\mathrm{NE} \times \mathrm{LE}}{\mathrm{NC} \times \mathrm{LC}}\right) \times 100 \quad (9)$$

where NE and NC are the numbers of germinated seeds watered by the effluent and the control (tap water), respectively. LE and LC are the average lengths of the radical of the germinated seeds watered by the effluent and the control, respectively.

Results and discussion

Effect of applied current density on the degradation rate of MTF

Current density is the most frequently pointed parameter that can affect COD removal during an electrooxidation process. To study the effect of this parameter on the electrochemical oxidation of MTF, different current densities rise from 5 to 40 mA cm^{-2} were applied on the BDD anode during 4 h of treatment. The initial solution contained 358 mg L^{-1} MTF (COD_0 = 900 mg L^{-1}) and 2 g L^{-1} Na_2SO_4 used as supporting electrolyte. The initial pH was fixed to 3, and the temperature was 293.15 K. Figure 1a illustrates the trend of COD values (%) with electrolysis time measured for different applied current densities. Actually, for all the current densities, the COD removal increased at the beginning of electrolysis and tended to stabilize after approximately 120 min. The highest COD abatement (66%) was obtained after 4 h when a current density of 30 mA cm^{-2} was applied due to the high production of $HO^{\bullet}$ radicals electrogenerated on the BDD surface from water discharge [Eq. (10)] (Rabaaoui et al. 2013a; Panizza et al. 2014).

$$\mathrm{BDD} + \mathrm{H_2O} \rightarrow \mathrm{BDD}(\mathrm{HO}^{\bullet}) + \mathrm{H}^+ + \mathrm{e}^- \quad (10)$$

However, for a current density higher than 30 mA cm^{-2}, the electrolysis efficiency decreases owing to parallel parasitic reactions, such as the oxidation of $HO^{\bullet}$ radicals to O_2 [Eq. (11)] and their dimerization to H_2O_2 [Eq. (12)] (Cavalcanti et al. 2013).

$$\mathrm{BDD}(\mathrm{HO}^{\bullet}) \rightarrow \mathrm{BDD} + 1/2\ \mathrm{O_2} + \mathrm{H}^+ + \mathrm{e}^- \quad (11)$$

$$\mathrm{BDD}(\mathrm{HO}^{\bullet}) \rightarrow \mathrm{BDD} + 1/2\ \mathrm{H_2O_2} \quad (12)$$

The organic matter removal was determined by the decrease in COD values during electrolyses. The reaction rate is given in Eq. (13) (Brahim et al. 2016).

$$r = -\frac{\mathrm{dCOD}}{\mathrm{d}t} = k[\mathrm{HO}^{\bullet}]^{\alpha}\mathrm{COD} = k_{\mathrm{obs}}\mathrm{COD} = \frac{Ak_{\mathrm{m}}}{V}\mathrm{COD} \quad (13)$$

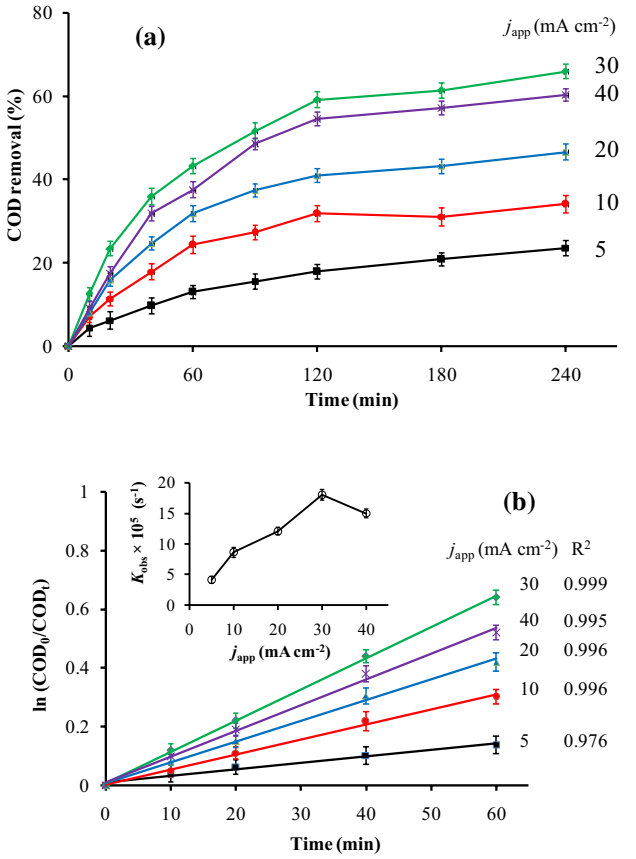

Fig. 1 Electrolysis of MTF at different applied current densities using a BDD anode $COD_0 = 900$ mg L^{-1}, $Na_2SO_4 = 2$ g L^{-1}, pH = 3 and $T = 293.15$ K. **a** removal of COD with time, **b** pseudo-first-order kinetic for COD

where α is the reaction order related to the adsorbed hydroxyl radicals concentration, k is the real rate constant, k_{obs} are the observed rate constant, k_m is the overall mass transport coefficient, A is the electrode area (m^2) and V is the volume of the treated solution (m^3).

The concentration of $HO^{\bullet}$ is assumed to be constant regardless of the applied current density and the treatment time since the electrode surface remained constant during the electrolyses.

Figure 1b presents the evolution of ln (COD_0/COD_t) with electrolysis time for all applied current densities. The linear regression procured in these plots was consistent with pseudo-first-order kinetics.

As shown in Fig. 1b, k_{obs} increases with j_{app} and reaches a maximum at 30 mA cm^{-2}. k_{obs} and k_m are proportional, resulting in a similar variation for k_m (Table 1). However, it is known that k_m depends only on temperature, leading to its increase with j_{app}, which can be explained through the comparison of j_{app} and $j_{lim,t}$. It can be observed in Fig. 2a that for a low value of j_{app} (5 mA cm^{-2}), $j_{lim,t}$ is always higher than j_{app}. The reaction is under charge transfer control. This behavior is consistent with CE values (CE = 1). For a high value of j_{app} (e.g. 40 mA cm^{-2}), $j_{lim,t}$ becomes lower than j_{app} after 40 min of electrolysis. Side reactions such as the generation of peroxodisulfate ($S_2O_8^{2-}$), sulfate radicals ($SO_4^{\bullet -}$) by supporting electrolyte decomposition [Eq. (14), (15)] and oxygen evolution [Eq. (16)] appeared, which leads to the decrease in the CE values (Vasilie et al. 2018).

$$2\,SO_4^{2-} \rightarrow S_2O_8^{2-} + 2\,e^- \quad (14)$$

$$SO_4^{2-} + HO^{\bullet} \rightarrow SO_4^{\bullet -} + HO^- \quad (15)$$

$$2\,H_2O \rightarrow O_2 + 4\,H^+ + 4\,e^- \quad (16)$$

The increase in O_2 bubbles amount produced and detached at the surface of the electrode with j_{app} improves the flow of species toward the electrode (Samet et al. 2006). It results in a decrease in the diffusion layer thickness and consequently an increase in k_m values (Table 1).

Moreover, in order to evaluate the influence of the applied current density on energy efficiency, energy consumption (Ec) was plotted as a function of the applied current density at different electrolysis times (Fig. 2b). When the current density increases from 5 to 40 mA cm^{-2}, the consumed energy is multiplied by a factor 25 $\left\{\text{Ec}\left(j = 40\text{ mA cm}^{-2}\right)/\text{Ec}\left(j = 5\text{ mA cm}^{-2}\right)\right\}$, whatever the electrolysis time is. This shows that Ec is independent of the composition of the reaction medium. Indeed, when organic matter decreases with electrolysis time according to Eq. (5), the corresponding Ec decreases, whereas, Ec relative to the side reactions [Eq. (14)–(16)] increases.

Effect of the supporting electrolyte nature and concentration on the degradation of MTF

Generally, supporting electrolyte used in an electrochemical oxidation reactor has two essential interests, namely increasing the conductivity of the solution and contributing to the degradation process by producing oxidizing species other than hydroxyl radicals (Salazar et al. 2016).

To study the effect of supporting electrolyte nature on the degradation of MTF, three supporting electrolytes (Na_2SO_4, NaCl and $NaNO_3$) at the same concentration of 2 g L^{-1} have been tested. A pH of 3 has been adjusted with H_2SO_4, HCl and/or HNO_3. Figure 3a illustrates the evolution of COD removal (%) with electrolysis time. Compared with NaCl and $NaNO_3$, Na_2SO_4 gives the highest COD removal percent (66% after 4 h). Under the same conditions, the use of NaCl or $NaNO_3$ instead of Na_2SO_4 leads only to 52 and 40% of COD removal, respectively. The obtained results can be attributed to the indirect oxidation of the organic matter via oxidative

Table 1 Electrolyses of MTF in 2 g L^{-1} Na_2SO_4 on the BDD anode. j_{lim4} and COD_4 are the limiting current density and COD removal measured after 4 h of electrolysis

j_{app} (mA cm^{-2})	5	10	20	30	40	
$K_{obs} \times 10^5$ (s^{-1})	4.1	8.6	12.0	18.0	14.9	$COD_0 = 900$ mg L^{-1}
$K_m \times 10^5$ (m s^{-1})	1.3	2.8	4.0	6.0	4.9	$T = 293.15$ K
j_{lim0} (mA cm^{-2})	14.1	30.3	43.4	65.1	53.1	pH = 3
j_{lim4} (mA cm^{-2})	10.5	19.6	22.6	21.7	20.6	
COD_0 (mg L^{-1})	300	600	900	1200		
$K_{obs} \times 10^5$ (s^{-1})	27.6	21.9	18.0	14.7		
$K_m \times 10^5$ (m s^{-1})	9.2	7.3	6.0	4.9		
$K_m\ COD_0 \times 10^3$ (g m^{-2} s^{-1})	27.6	43.8	54.0	58.8		$j_{app} = 30$ mA cm^{-2}
$K_m\ COD_4 \times 10^3$ (g m^{-2} s^{-1})	5.5	12.2	18.0	25.4		$T = 293.15$ K
j_{lim0} (mA cm^{-2})	33.2	52.8	65.1	70.9		pH = 3
COD_4 removal (%)	80	72	66	57		
T (K)	293.15	313.15	328.15	343.15		
ln $k^{\ddagger}$	− 38.06	− 37.93	− 37.74	− 37.54		$COD_0 = 900$ mg L^{-1}
$\Delta G^{\ddagger^\circ}$ (kJ mol^{-1})	92.71	98.70	102.91	107.05		$j_{app} = 30$ mA cm^{-2}
$\Delta H^{\ddagger^\circ}$ (kJ mol^{-1})	8.65					pH = 3
$\Delta S^{\ddagger^\circ}$ (J mol^{-1} K^{-1})	− 287.24					

mediators such as $S_2O_8^{2-}$ and HClO, as the predominant active chlorine species at pH = 3, electrogenerated at the anode surface. Since the oxidative power of $S_2O_8^{2-}$ is higher than that of HClO according to their standard redox potentials $\left(E^0_{(S_2O_8^{2-}/SO_4^{2-})} = 2.01\ V/SHE \text{ and } E^0_{(HClO/Cl^-)} = 1.50\ V/SHE\right)$, the higher performance of the electrode is obtained when using Na_2SO_4.

Since NO_3^- is an inert species, when using $NaNO_3$ as a supporting electrolyte, only direct oxidation via $HO^\bullet$ radicals take place. Thus, it is possible to evaluate the contribution of indirect oxidation in the removal of organic matter. From Fig. 3a, it can be seen that after 4 h of electrolysis, the indirect oxidation enhanced the COD removal (%) by 26 and 14% when using Na_2SO_4 and NaCl, respectively.

To evaluate the effect of the supporting electrolyte concentration on the degradation efficiency of MTF, electrolyses were carried out at a current density of 30 mA cm^{-2} using different amounts of Na_2SO_4 (1–8 g L^{-1}). COD removal percent and energy consumption measured after 4 h of treatment were calculated (Fig. 3b). It was found that the increase in Na_2SO_4 concentration from 1 to 8 g L^{-1} leads to the increase in the COD removal percent from 59.0 to 79.2%. This result is related to the increase in the $S_2O_8^{2-}$ concentration generated according to Eq. (14). $S_2O_8^{2-}$ is an oxidizing species which contributes in the oxidation of MTF and its by-products.

To further explain this result, it is necessary to take into account the variation of the solution conductivity as well as the energy consumption for each experiment. In fact, the increase in the supporting electrolyte concentration was followed by an enhancement in the electrical conductivity from 1.89 mS cm^{-1} (for 1 g L^{-1} of Na_2SO_4) to 3.07, 5.90, 7.07 and 10.55 mS cm^{-1} for 2, 4, 6 and 8 g L^{-1} of Na_2SO_4, respectively. Consequently, the energy consumption dropped from 51.48 to 23.72 kW h m^{-3} (Fig. 3b).

As illustrated in Fig. 3b, the influence of Na_2SO_4 concentration weakened gradually or even became insignificant when the electrolyte concentration reached 6 g L^{-1}. In fact, after 4 h of electrolysis, only an improvement of 2% of COD removal percent was obtained when Na_2SO_4 concentration increased from 6 to 8 g L^{-1}. Although 6 g L^{-1} Na_2SO_4 seems to be the most adequate concentration, from an environmental point of view, it is necessary to use a small amount of Na^+ ions since sodium is a very mobile ion, leading to groundwater pollution (Grasso et al. 2005).

Effect of the initial concentration of MTF

For industrial wastewater treatment plants, it is important to take into account the study of the effect of organic pollutants concentration. Thus, the electrochemical oxidation of MTF has been studied at different initial concentrations (COD_0 between 300 and 1200 mg L^{-1}).

The results given in Fig. 4 and Table 1 indicate that the increase in COD_0 from 300 to 1200 mg L^{-1} led to a decrease in COD removal percent. For the higher COD_0, at most 57% of COD removal was achieved after 4 h of electrolysis. However, for an initial COD of 300 mg L^{-1}, 80% of COD removal was obtained. This result indicates that the degradation process is limited by charge transfer whatever COD_0.

It is clear that the complete elimination of COD was not achieved in any test, even for a low concentration of MTF. This behavior is related to the inhibitory oxidative effect of some intermediates such as ammonia, amines, amidines and urea derivatives (Badran et al. 2019a, b). When COD_0 increased, k_m values obtained from k_{obs} decreased (Table 1),

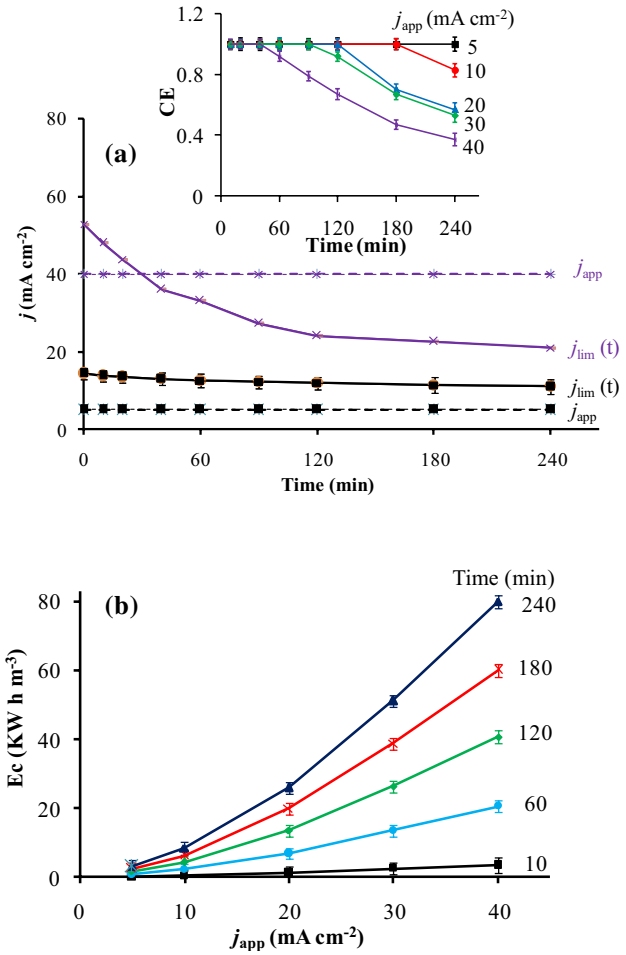

Fig. 2 Comparison between j_{app} and j_{limt} during the electrolysis of MTF. $COD_0 = 900$ mg L^{-1}; $Na_2SO_4 = 2$ g L^{-1}; pH = 3 and $T = 293.15$ K. **a** Effect of j_{app} on the trends of current efficiency. **b** Effect of j_{app} on the energy consumption

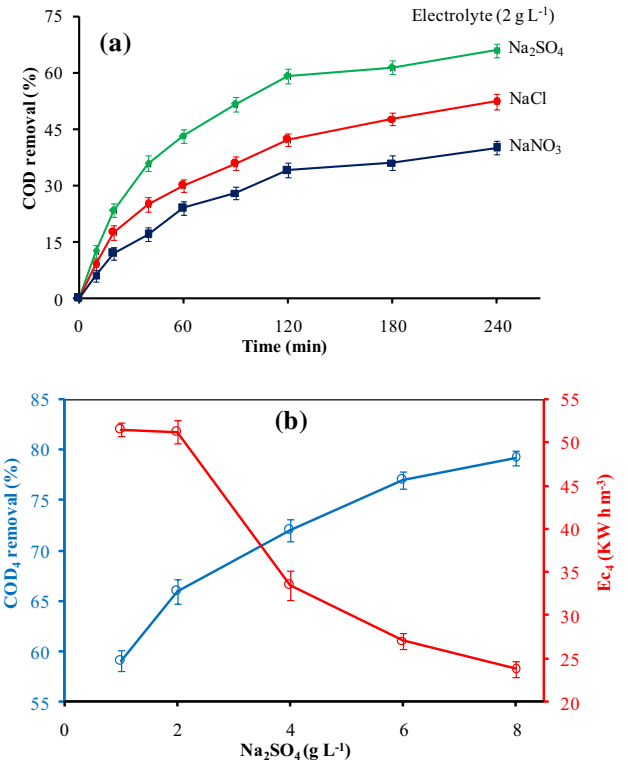

Fig. 3 **a** Effect of Na_2SO_4 concentration on the COD removal and energy consumption after 4 h of MTF electrolysis, **b** Effect of the electrolyte nature on the COD removal. $COD_0 = 900$ mg L^{-1}, $j_{app} = 30$ mA cm^{-2}, pH = 3 and $T = 293.15$ K

which can be explained by a decrease in the oxygen formation rate. However, the total mass transport rates ($k_m COD_t$) raised, and therefore when COD_0 increased, the degradation rate greatly increased. This can be interpreted in terms of the increase in the diffusion flux of organic matter to the surface of the electrode. j_{lim0} values (higher than j_{app} whatever the initial COD) are in accordance with the charge transfer control process at the beginning of electrolysis.

Effect of temperature

Figure 5a shows the variation of COD removals percentage during the electrolysis of MTF solutions ($COD_0 = 900$ mg L^{-1}) at 293.15, 313.15, 328.15 and 343.15 K under an applied current density of 30 mA cm^{-2} and initial pH value fixed to 3. The increase in temperature favors MTF oxidation. Indeed, after 4 h of treatment, COD removal (%) increased from 66 to 91% with the increase in the temperature from 293.15 to 343.15 K. This result is probably due to the electro-generation of inorganic oxidant agent ($S_2O_8^{2-}$) from the supporting electrolyte [Eq. (14)]. This reagent constitutes a new source for the indirect oxidation of organic compounds whose rate increases with temperature (Brahim et al. 2016). Furthermore, the rise in temperature leads to a decrease in the viscosity of the medium and, hence, the increase in the rate of organic matter diffusion toward the electrode surface. This finding is in agreement with those found in earlier investigations about the oxidation of benzoquinone (Panizza 2014) and acid yellow (Rodriguez et al. 2009) on BDD anode.

The relationship between the reaction temperature and k_{obs} are expressed according to the Arrhenius law as follows [Eq. (17)]:

$$k_{obs} = Ae^{-\frac{E_a}{RT}} \quad (17)$$

where A is the frequency factor, E_a is the apparent global activation energy (J mol^{-1}), R is the ideal gas constant (8.314 J mol^{-1} K^{-1}) and T is the absolute temperature (K).

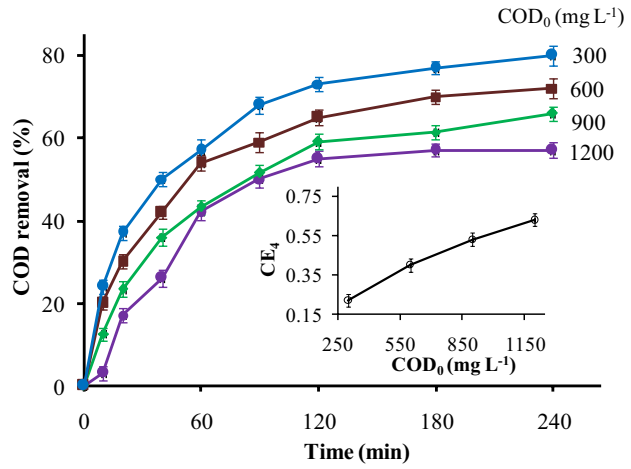

Fig. 4 Effect of the initial concentration of MTF on the COD removal during the electrolysis. The small graph shows the current efficiency measured after 4 h of electrolysis. $Na_2SO_4 = 2$ g L^{-1}, $j_{app} = 30$ mA cm^{-2}, pH = 3 and $T = 293.15$ K

From Fig. 5b, COD removal follows a pseudo-first-order kinetics and the k_{obs} increased with temperature, being 0.650, 0.835, 1.014 and 1.221 h^{-1} at 293.15, 313.15, 328.15 and 343.15 K, respectively. E_a and A were determined from the slope ($-E_a/R$) and the intercept (ln A) as 10.5 kJ mol^{-1} and 47.84 h^{-1}, respectively. It can be suggested that the limiting step of MTF oxidation is controlled by diffusion since E_a for a homogeneous diffusion-controlled reaction is typically less than 40 kJ mol^{-1} (Gargouri et al. 2013).

On the other hand, according to the Eyring–Polanyi model, k_{obs} can be related to the standard Gibbs energy of activation $\Delta G^{\#\circ}$ by:

$$k_{obs} = \kappa \frac{k_B T}{h} \exp\left(-\frac{\Delta G^{\#\circ}}{RT}\right) \quad (18)$$

where κ is the transmission coefficient ($0 \le \kappa \le 1$) which is considered to be close to unity in most cases, k_B is the Boltzmann constant and h is the Planck's constant.

$\Delta G^{\#\circ}$ can be expressed by Eq. (19): (Ptáček et al. 2018)

$$\Delta G^{\#\circ} = -RT \ln K^{\#} = \Delta H^{\#\circ} - T\Delta S^{\#\circ} \quad (19)$$

where $K^{\#}$ is the equilibrium constant of the formation of the activated complex of the reaction, whose value can be calculated using the following equation:

$$K^{\#} = \frac{k_{obs} \mathcal{N} h}{RT} \quad (20)$$

where $\mathcal{N}$ is the Avogadro's number.

The enthalpy of activation ($\Delta H^{\#\circ}$) and the entropy of activation ($\Delta S^{\#\circ}$) were determined by plotting ln $K^{\#}$ versus 1/T.

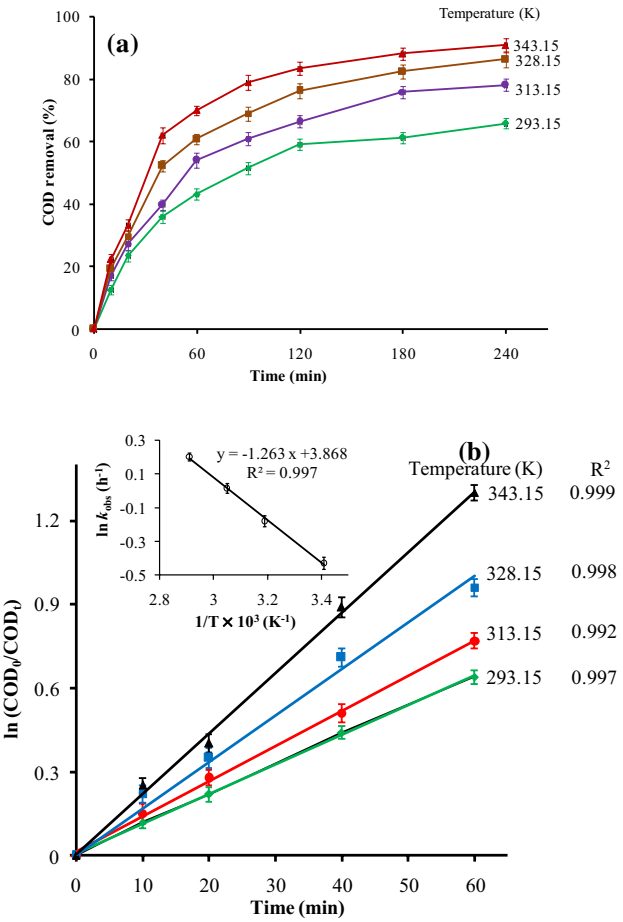

Fig. 5 **a** Effect of temperature on the COD removal during the electrolysis of MTF, **b** Pseudo-first-order kinetic for COD. COD$_0$ = 900 mg L^{-1}, $Na_2SO_4 = 2$ g L^{-1}, $j_{app} = 30$ mA cm^{-2} and pH = 3

$$\ln K^{\#} = -\frac{\Delta H^{\#\circ}}{RT} + \frac{\Delta S^{\#\circ}}{R} \quad (21)$$

The results are given in Table 1, revealing that $\Delta H^{\#\circ}$ is close to E_a. Theoretically, E_a is related to $\Delta H^{\#\circ}$ by the following equation.

$$E_a = \Delta H^{\#\circ} - RT \quad (22)$$

Effect of the NaCl concentration on the degradation rate of MTF

The chloride salts of sodium (NaCl) play an important role through the indirect electrochemical oxidation of organic pollutants. It has been widely used as a decontaminant agent for aqueous effluents because it can provide a media with more powerful oxidizing species during the electrolysis such as chlorine (Cl_2), hypochlorous acid (HClO) and

hypochlorite (ClO^-) (Panizza and Cerisola 2009), produced by the oxidation of chloride ions, according to the following reactions [Eq. (23)–(26)]:

$$2\,Cl^- \rightarrow Cl_2 + 2\,e^- \quad (23)$$

$$Cl^- + 2\,OH^- \rightarrow ClO^- + H_2O + 2\,e^- \quad (24)$$

$$Cl_2 + H_2O \rightarrow HClO + H^+ + Cl^- \quad (25)$$

$$HClO \rightarrow H^+ + ClO^- \quad (26)$$

These species are able to oxidize organic compounds by promoting the degradation rates.

One of the first articles reporting on the catalytic effect of chloride ions in organic pollutants oxidation was published by Comninellis and Nerini (Comninellis and Nerini 1995). These authors have shown that the presence of NaCl catalyzes the anodic oxidation of phenol by the generation of ClO^- using Ti/IrO_2 anode.

Another explanation of the mediating role of chloride ions has been proposed by Panizza et al. (Panizza et al. 2007). They compared the direct and indirect electrolyses of methylene blue solution and proved that the latter facilitates not only mineralization but also the discoloration of the solution and overcomes the mass transfer limitations.

In the present study, the effect of NaCl on the degradation rate of MTF was evaluated using a current density of 30 mA cm^{-2} and different amounts of salt. The results obtained in Fig. 6 show that the presence of chloride ions improves the performance of the electrode. In fact, without NaCl, only 66% of COD was removed, whereas, in the presence of 0.4 or 0.8 g L^{-1} of the salt, the COD removal was 83.43 and 92.74%, respectively. An amount of NaCl greater than 0.8 g L^{-1} does not significantly improve the rate of COD removal.

It is worthy to note that even when the use of NaCl allows the increase in the efficiency of the degradation and notably reduces the process costs, the NaCl added to the effluent should be used in moderate amounts to minimize the generation of Cl_2, a toxic molecule known for its carcinogenic properties (Jardak et al. 2016). For this reason, it is recommended to use 0.8 g L^{-1} NaCl.

Effect of pH

Solution pH is one of the main factors that must be optimized to ensure the electrochemical oxidation efficiency of electroactive compounds. While some electrolyses are favored in an acidic aqueous medium (Scialdone et al. 2008; Rabaaoui et al. 2013b), others are privileged in alkaline or neutral solution (Lissens et al. 2003; Gargouri et al. 2013). Other studies have confirmed the independence of the process on pH (Ellouze et al. 2016), which depends on several factors, such as the chemical property and reactivity of the compound, the supporting electrolyte nature and the electrode material (Editorial 2009).

The electrolysis of MTF on the BDD electrode is favored in an acidic medium as illustrated by the evolution of k_{obs} with pH (Fig. 7). At the end of electrolysis, COD removal increased from 33 to 75% when the pH decreased from 9 to 2 (Fig. 7). In fact, the amount of $HO^\bullet$ produced on the BDD surface [Eq. (10)] in an acidic medium is more important than that obtained in an alkaline medium (Enache et al. 2009). Moreover, the increase in the pH decreases the O_2 over-potential, and consequently, the O_2 production becomes easier (Chen et al. 2003; Scialdone et al. 2008). This concurrent reaction decreases the COD removal efficiency.

Electrolysis under optimal conditions

The electrolysis of MTF was carried out under optimal conditions (COD_0 = 900 mg L^{-1}, Na_2SO_4 = 2 g L^{-1}, NaCl = 0.8 g L^{-1}, j_{app} = 30 mA cm^{-2}, pH = 2 and T = 343.15 K). The degradation kinetics of MTF was followed by the measurement of COD and MTF concentration. The quantification of MTF was performed by the SWV technique (Fig. 8a). The results given in Fig. 8b indicate that during electrolysis, the decrease in MTF concentration is faster than that of COD. MTF molecules disappear completely after 2 h where COD removal percent was about 90%. As COD removal evolution with time electrolysis, the linear regression obtained from the evolution of ln ($[MTF]_0$ / $[MTF]_t$)with electrolysis time was consistent with a pseudo-first-order kinetics.

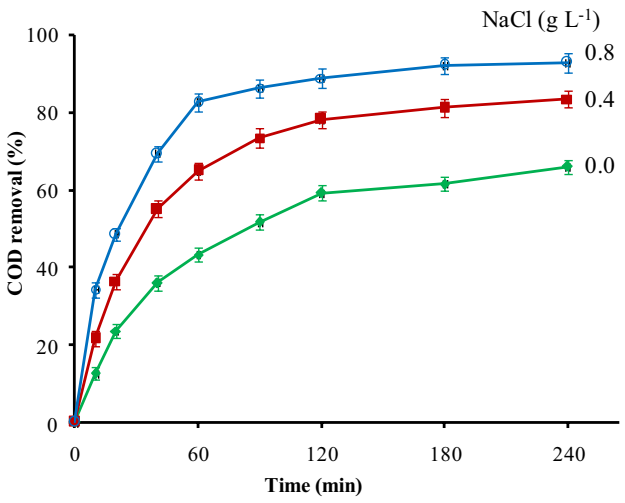

Fig. 6 Effect of NaCl concentration on the COD removal during the electrolysis of MTF. COD_0 = 900 mg L^{-1}, Na_2SO_4 = 2 g L^{-1}, j_{app} = 30 mA cm^{-2}, pH = 3 and T = 293.15 K

These experimental results have proven that the electrochemical oxidation is an effective method for the treatment of water containing MTF.

Phytotoxicity assessment

The reuse of treated wastewater for agricultural irrigation has become very important due to the scarcity of natural water resources. This has encouraged many countries to develop local regulations to control the quality of water for the reuse to reduce health and environmental risks (Drechsel et al. 2015). Therefore, phytotoxicity tests assess the toxicity profile of a substance measuring the response of a living organism. There are many widely accepted benefits of using germination rate and root elongation as a rapid phytotoxicity method such as simplicity, high sensitivity, cost-effectiveness and suitability (Wang et al. 2001).

In the present work, Fenugreek and Lucerne seeds were applied for the irrigation tests with different treated water samples during the electrolysis of solution containing MTF ($COD_0 = 900$ mg L^{-1}, $Na_2SO_4 = 2$ g L^{-1}, $j_{app} = 30$ mA cm^{-2}, pH = 2 and $T = 293.15$ K). The results illustrated in Fig. 9A reveal different GI percent depending on the quality of water. Irrigation with tap water with or without MTF gives 100% GI, indicating that the drug has no effects on the growth of both plants (Fig. 9A a). The lower GI% (8% for Fenugreek and 5% for Lucerne) was obtained with distilled water containing only Na_2SO_4 2 g L^{-1} due to the water's lack of mineral salts (Fig. 9A b). Since MTF molecule contains nitrogen in its structure, adding this molecule to distilled water slightly improves GI% (30% for Fenugreek and 24% for Lucerne) (Fig. 9A c). This behavior has also been observed by Eggen and Lillo (2012). During electrolysis, GI% increased gradually attaining 89% for Fenugreek and 80% for Lucerne after 4 h of treatment (Fig. 9A d–g). Such increase shows the gradual production of nitrate ions from the degradation of the MTF molecules as presented by Fig. 9B. NO_3^- and NH_4^+ concentrations were followed during electrolysis. The two ions were accumulated rapidly during the early time of treatment and then reached steady-state values from 60 min. In this case, the $\frac{NH_4^+}{NO_3^-}$ ratio is maintained above 22. The formation of nitrate ions can be attributed to the oxidation of ammonium ions on the BDD surface.

Based on the results of the performed tests, it is clear that no phytotoxicity effect on Fenugreek and Lucerne seeds existed. On the contrary, the presence of this drug in water improves the growth of these two plants. However, its

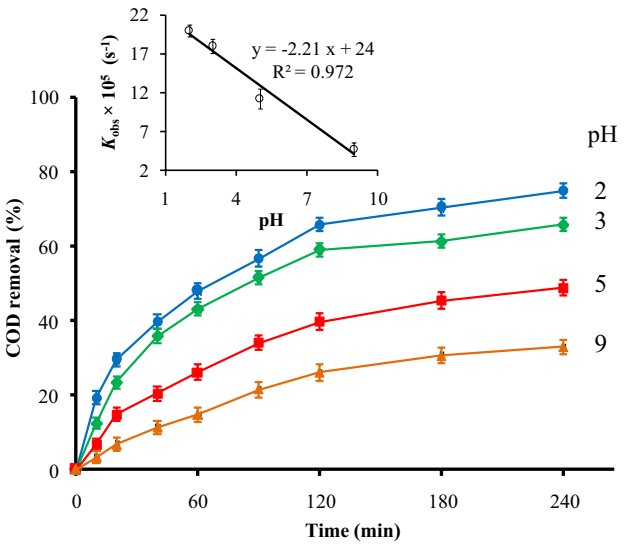

Fig. 7 Effect of pH on the COD removal during the electrolysis of MTF. $COD_0 = 900$ mg L^{-1}, $Na_2SO_4 = 2$ g L^{-1}, $j_{app} = 30$ mA cm^{-2} and $T = 293.15$ K

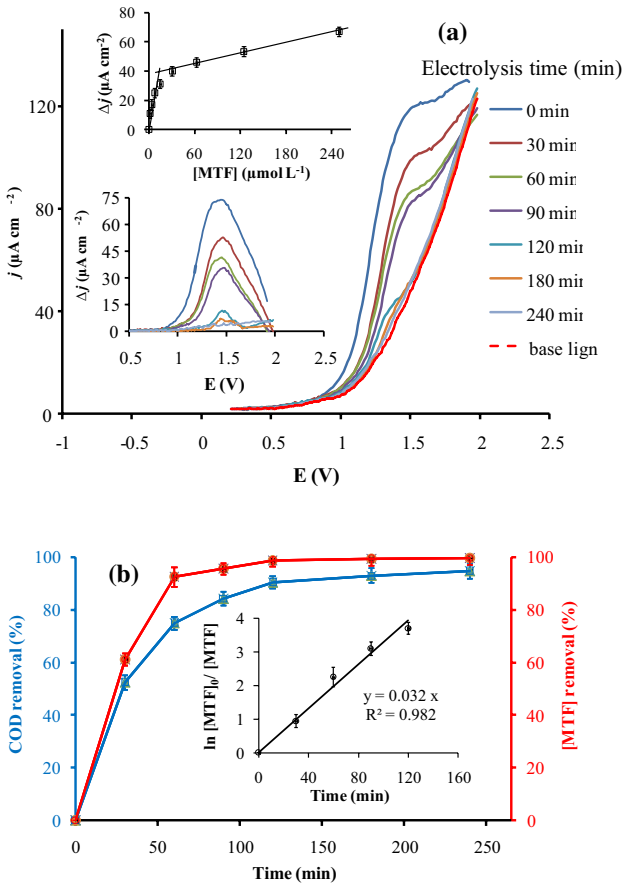

Fig. 8 **a** Analysis of MTF by SWV during electrolysis. Δ *j:* voltammograms after subtraction of the blank current (base line). $COD_0 = 900$ mg L^{-1}; pH = 12.5; $Na_2SO_4 = 2$ g L^{-1}; NaCl = 0.8 g L^{-1}; $j_{app} = 30$ mA cm^{-2}; $T = 293.15$ K; $f = 100$ Hz; $\Delta E_a = 50$ mV and $\Delta E_s = 5$ mV. **b** Evolution of the MTF concentration and COD removal during the electrolysis of MTF under optimal conditions

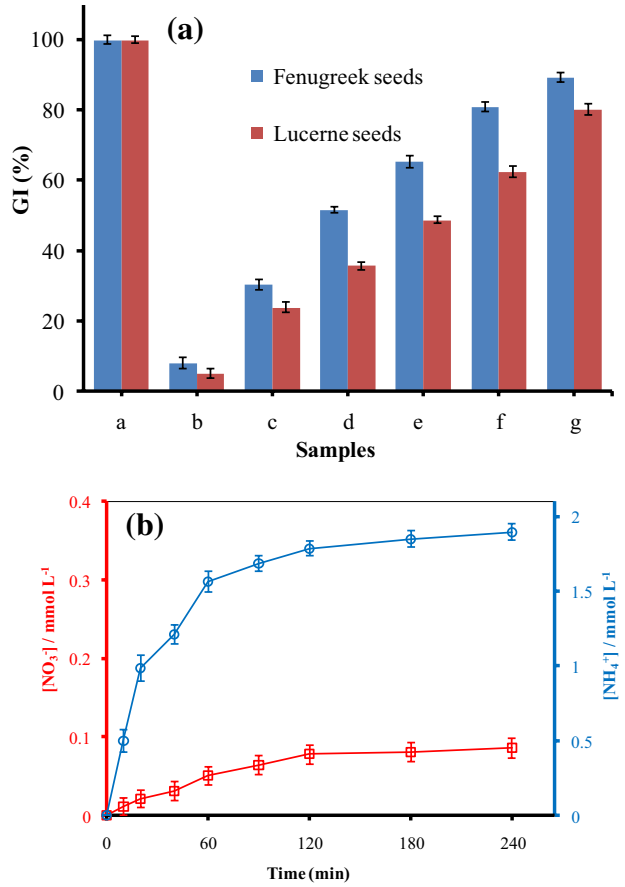

Fig. 9 **A** Phytotoxicity of water containing MTF (COD_0 = 900 mg L^{-1}) on Fenugreek and Lucerne seeds at different electrolysis times. *a* Tap water with or without MTF, *b* distilled water + Na_2SO_4 = 2 g L^{-1}, *c* distilled water + Na_2SO_4 = 2 g L^{-1} + MTF (COD_0 = 900 mg L^{-1}), *d*–*g* Treated water after 1, 2, 3 and 4 h of electrolysis, respectively. **B** Concentration of NH_4^+ and NO_3^- ions accumulated during the electrolysis of MTF (COD_0 = 900 mg L^{-1}) at pH = 2, Na_2SO_4 = 2 g L^{-1} and T = 343.15 K

presence in the plant represents a health problem for humans and animals. Therefore, the degradation of MTF in water is necessary and beneficial for irrigation use.

Conclusion

The electrolysis of solutions containing the antidiabetic metformin (MTF) using a BDD anode was proven to be an efficient process for the complete removal of this drug. Significant decrease in COD and complete removal of the drug were observed during electrolysis under optimal conditions (j_{app} = 30 mA cm^{-2}, Na_2SO_4 = 2 g L^{-1}, NaCl = 0.8 g L^{-1}, pH = 2 and T = 343.15 k). The kinetic decrease in MTF molecules and COD shows that it follows a pseudo-first-order. Moreover, the addition of NaCl in the aqueous electrolytic solution promotes the degradation of the main compound due to the generation of species with a higher oxidation potential such as active chlorine.

The phytotoxicity tests were also carried out using Fenugreek and Lucerne seeds. It was observed that despite the beneficial effect of MTF on the growth of the plant, its presence in the stems and leaves of these plants has a problem of toxicity for consumers. It is therefore necessary to treat the water containing this drug before its use in agriculture.

Acknowledgements The authors would like to express their thanks to Professor Mohamed-Faouzi Ahmadi (Laboratoire de Toxicologie Microbiologie Environnementale et Santé (LR17ES06), Sciences Faculty of Sfax, University of Sfax, Tunisia) for reading and comments made on this paper.

Declarations

Conflict of interest On behalf of all authors, the corresponding authors states that there is no conflict of interest.

Ethical approval This article does not contain any studies with human participants or animals performed by any of the authors.

References

Adel Niaei H, Rostamizadeh M (2020) Adsorption of metformin from an aqueous solution by Fe-ZSM-5 nano-adsorbent: isotherm, kinetic and thermodynamic studies. J Chem Thermodyn 142:106003. https://doi.org/10.1016/j.jct.2019.106003

Alnajjar M, Hethnawi A, Nafie G et al (2019) Silica-alumina composite as an effective adsorbent for the removal of metformin from water. J Environ Chem Eng 7:1–10. https://doi.org/10.1016/j.jece.2019.102994

Badran I, Hassan A, Manasrah AD, Nassar NN (2019a) Experimental and theoretical studies on the thermal decomposition of metformin. J Therm Anal Calorim 138:433–441. https://doi.org/10.1007/s10973-019-08213-9

Badran I, Manasrah AD, Nassar NN (2019b) A combined experimental and density functional theory study of metformin oxy-cracking for pharmaceutical wastewater treatment. RSC Adv 9:13403–13413. https://doi.org/10.1039/c9ra01641d

Balasubramani K, Sivarajasekar N, Naushad M (2020) Effective adsorption of antidiabetic pharmaceutical (metformin) from aqueous medium using graphene oxide nanoparticles: Equilibrium and statistical modelling. J Mol Liq 301:112426. https://doi.org/10.1016/j.molliq.2019.112426

Brahim BM, Ammar HB, Abdelhédi R, Samet Y (2016) Electrochemical removal of the insecticide imidacloprid from water on a boron-doped diamond and Ta/PbO_2 anodes using anodic oxidation process. Korean J Chem Eng 33:2602–2609. https://doi.org/10.1007/s11814-016-0128-0

Briones RM, Sarmah AK, Padhye LP (2016) A global perspective on the use, occurrence, fate and effects of anti-diabetic drug metformin in natural and engineered ecosystems. Environ Pollut 219:1007–1020. https://doi.org/10.1016/j.envpol.2016.07.040

Carbuloni CF, Savoia JE, Santos JSP et al (2020) Degradation of metformin in water by TiO_2–ZrO_2 photocatalysis. J Environ Manage 262:110347. https://doi.org/10.1016/j.jenvman.2020.110347

Cavalcanti EB, Garcia-Segura S, Centellas F, Brillas E (2013) Electrochemical incineration of omeprazole in neutral aqueous medium using a platinum or boron-doped diamond anode: Degradation kinetics and oxidation products. Water Res 47:1803–1815. https://doi.org/10.1016/j.watres.2013.01.002

Chen X, Chen G, Gao F, Yue PL (2003) High-performance Ti/BDD electrodes for pollutant oxidation. Environ Sci Technol 37:5021–5026. https://doi.org/10.1021/es026443f

Chinnaiyan P, Thampi SG, Kumar M, Balachandran M (2019) Photocatalytic degradation of metformin and amoxicillin in synthetic hospital wastewater: effect of classical parameters. Int J Environ Sci Technol 16:5463–5474. https://doi.org/10.1007/s13762-018-1935-0

Cho NH, Shaw JE, Karuranga S et al (2018) IDF Diabetes Atlas: Global estimates of diabetes prevalence for 2017 and projections for 2045. Diabetes Res Clin Pract 138:271–281. https://doi.org/10.1016/j.diabres.2018.02.023

Comninellis C, Nerini A (1995) Anodic oxidation of phenol in the presence of NaCl for wastewater treatment. J Appl Electrochem 25:23–28. https://doi.org/10.1007/BF00251260

De la Cruz N, Esquius L, Grandjean D et al (2013) Degradation of emergent contaminants by UV, UV/H2O2 and neutral photo-Fenton at pilot scale in a domestic wastewater treatment plant. Water Res 47:5836–5845. https://doi.org/10.1016/j.watres.2013.07.005

Dolatabadi M, Ahmadzadeh S (2019) A rapid and efficient removal approach for degradation of metformin in pharmaceutical wastewater using electro-Fenton process; optimization by response surface methodology. Water Sci Technol 80:685–694. https://doi.org/10.2166/wst.2019.312

Drechsel P, Qadir M, Wichelns D (2015) Wastewater: Economic asset in an urbanizing world. Wastewater: Economic Asset in an Urbanizing World 1–282. https://doi.org/10.1007/978-94-017-9545-6

Editorial G (2009) Membrane reactors—part I. Technology. https://doi.org/10.1002/apj

Eggen T, Lillo C (2012) Antidiabetic II drug metformin in plants: uptake and translocation to edible parts of cereals, oily seeds, beans, tomato, squash, carrots, and potatoes. J Agric Food Chem 60:6929–6935. https://doi.org/10.1021/jf301267c

Elizalde-Velázquez GA, Gómez-Oliván LM (2020) Occurrence, toxic effects and removal of metformin in the aquatic environments in the world: recent trends and perspectives. Sci Total Environ. https://doi.org/10.1016/j.scitotenv.2019.134924

Ellouze S, Panizza M, Barbucci A et al (2016) Ferulic acid treatment by electrochemical oxidation using a BDD anode. J Taiwan Inst Chem Eng 59:132–137. https://doi.org/10.1016/j.jtice.2015.09.008

Enache TA, Chiorcea-Paquim AM, Fatibello-Filho O, Oliveira-Brett AM (2009) Hydroxyl radicals electrochemically generated in situ on a boron-doped diamond electrode. Electrochem Commun 11:1342–1345. https://doi.org/10.1016/j.elecom.2009.04.017

Escudero A, Hunter C, Roberts J et al (2020) Pharmaceuticals removal and nutrient recovery from wastewaters by Chlamydomonas acidophila. Biochem Eng J 156:107517. https://doi.org/10.1016/j.bej.2020.107517

Gabr RQ, El-Sherbeni AA, Ben-Eltriki M, El-Kadi AO, Brocks DR (2017) Pharmacokinetics of metformin in the rat: assessment of the effect of hyperlipidemia and evidence for its metabolism to guanylurea. Can J Physiol Pharmacol 95(5):530–538. https://doi.org/10.1139/cjpp-2016-0329

García J, García-Galán MJ, Day JW et al (2020) A review of emerging organic contaminants (EOCs), antibiotic resistant bacteria (ARB), and antibiotic resistance genes (ARGs) in the environment: Increasing removal with wetlands and reducing environmental impacts. Biores Technol 307:123228. https://doi.org/10.1016/j.biortech.2020.123228

Gargouri OD, Samet Y, Abdelhedi R (2013) Electrocatalytic performance of PbO_2 films in the degradation of dimethoate insecticide. Water SA 39:31–38. https://doi.org/10.4314/wsa.v39i1.5

Grasso D, Strevett K, Pesari H (2005) Impact of sodium and potassium on environmental systems. J Environ Syst 22:297–323. https://doi.org/10.2190/rrnd-6y9q-jn16-06nd

Hejzlar J, Kopáček J (1990) Determination of low chemical oxygen demand values in water by the dichromate semi-micro method. Analyst 115:1463–1467. https://doi.org/10.1039/AN9901501463

IDF Diabetes Atlas (2019) No title international diabetes federation. IDF Diabetes Atlas, 9th edn. International Diabetes Federation, Brussels. http://www.diabetesatlas.org/

Jardak K, Dirany A, Drogui P, El Khakani MA (2016) Electrochemical degradation of ethylene glycol in antifreeze liquids using boron doped diamond anode. Sep Purif Technol 168:215–222. https://doi.org/10.1016/j.seppur.2016.05.046

Kairigo P, Ngumba E, Sundberg LR et al (2020) Occurrence of antibiotics and risk of antibiotic resistance evolution in selected Kenyan wastewaters, surface waters and sediments. Sci Total Environ 720:137580. https://doi.org/10.1016/j.scitotenv.2020.137580

Koagouw W, Ciocan C (2018) Impact of Metformin and Increased Temperature on Blue Mussels Mytilus edulis—evidence for Synergism. J Shellfish Res 37:467–474. https://doi.org/10.2983/035.037.0301

Lee JW, Shin YJ, Kim H et al (2019) Metformin-induced endocrine disruption and oxidative stress of Oryzias latipes on two-generational condition. J Hazard Mater 367:171–181. https://doi.org/10.1016/j.jhazmat.2018.12.084

Lissens G, Pieters J, Verhaege M et al (2003) Electrochemical degradation of surfactants by intermediates of water discharge at carbon-based electrodes. Electrochim Acta 48:1655–1663. https://doi.org/10.1016/S0013-4686(03)00084-7

Lović J, Lađarević J, Mijin D et al (2019) Electrochemical stability of metformin in NaHCO3 and Na2SO4 water solution at Au, GC and

IrOx electrodes. J Serb Chem Soc 84:1319–1327. https://doi.org/10.2298/JSC190731091L
Malin SK, Kashyap SR (2014) Effects of metformin on weight loss: potential mechanisms. Curr Opin Endocrinol Diabetes Obes 21:323–329. https://doi.org/10.1097/MED.0000000000000095
Mallik R, Chowdhury TA (2018) Metformin in cancer. Diabetes Res Clin Pract 143:409–419. https://doi.org/10.1016/j.diabres.2018.05.023
Niemuth NJ, Jordan R, Crago J et al (2015) Metformin exposure at environmentally relevant concentrations causes potential endocrine disruption in adult male fish. Environ Toxicol Chem 34:291–296. https://doi.org/10.1002/etc.2793
Orata ED, De Leon PDP, Doma BT (2019) Degradation of metformin in water using electro-Fenton process. IOP Confer Ser: Earth Environ Sci. https://doi.org/10.1088/1755-1315/344/1/012007
Ottmar KJ, Colosi LM, Smith JA (2010) Development and application of a model to estimate wastewater treatment plant prescription pharmaceutical influent loadings and concentrations. Bull Environ Contam Toxicol 84:507–512. https://doi.org/10.1007/s00128-010-9990-3
Panizza M (2014) Anodic oxidation of benzoquinone using diamond anode. Environ Sci Pollut Res 21:8451–8456. https://doi.org/10.1007/s11356-014-2782-2
Panizza M, Barbucci A, Ricotti R, Cerisola G (2007) Electrochemical degradation of methylene blue. Sep Purif Technol 54:382–387. https://doi.org/10.1016/j.seppur.2006.10.010
Panizza M, Cerisola G (2009) Direct and mediated anodic oxidation of organic pollutants. Chem Rev 109:6541–6569. https://doi.org/10.1021/cr9001319
Panizza M, Dirany A, Sirés I et al (2014) Complete mineralization of the antibiotic amoxicillin by electro-Fenton with a BDD anode. J Appl Electrochem 44:1327–1335. https://doi.org/10.1007/s10800-014-0740-9
Papageorgiou M, Zioris I, Danis T et al (2019) Comprehensive investigation of a wide range of pharmaceuticals and personal care products in urban and hospital wastewaters in Greece. Sci Total Environ 694:133565. https://doi.org/10.1016/j.scitotenv.2019.07.371
Patil TR, Patil ST, Patil SPA (2018) Antimicrobial Potential of Metformin. Int J Pharmacogn Phytochem Res 10:279–283. https://doi.org/10.25258/phyto.10.7.2
Perret A, Haenni W, Skinner N et al (1999) Electrochemical behavior of synthetic diamond thin film electrodes. Diam Relat Mater 8:820–823. https://doi.org/10.1016/s0925-9635(98)00280-5
Ptáček P, Šoukal F, Opravil T (2018) Introduction to the transition state theory. Introd Effect Mass Activ Complex Discuss Wave Funct Instanton. https://doi.org/10.5772/intechopen.78705
Rabaaoui N, Moussaoui Y, Allagui MS et al (2013a) Anodic oxidation of nitrobenzene on BDD electrode: variable effects and mechanisms of degradation. Sep Purif Technol 107:318–323. https://doi.org/10.1016/j.seppur.2013.01.047
Rabaaoui N, Saad MEK, Moussaoui Y et al (2013b) Anodic oxidation of o-nitrophenol on BDD electrode: variable effects and mechanisms of degradation. J Hazard Mater 250–251:447–453. https://doi.org/10.1016/j.jhazmat.2013.02.027
Rodrigo MA, Michaud PA, Duo I et al (2001) Oxidation of 4-chlorophenol at boron-doped diamond electrode for wastewater treatment. J Electrochem Soc 148:D60. https://doi.org/10.1149/1.1362545
Rodriguez J, Rodrigo MA, Panizza M, Cerisola G (2009) Electrochemical oxidation of Acid Yellow 1 using diamond anode. J Appl Electrochem 39:2285–2289. https://doi.org/10.1007/s10800-009-9880-8
Salazar C, Contreras N, Mansilla HD et al (2016) Electrochemical degradation of the antihypertensive losartan in aqueous medium by electro-oxidation with boron-doped diamond electrode. J Hazard Mater 319:84–92. https://doi.org/10.1016/j.jhazmat.2016.04.009
Samet Y, Elaoud SC, Ammar S, Abdelhedi R (2006) Electrochemical degradation of 4-chloroguaiacol for wastewater treatment using PbO_2 anodes. J Hazard Mater 138:614–619. https://doi.org/10.1016/j.jhazmat.2006.05.100
Sanchez-Rangel E, Inzucchi SE (2017) Metformin: clinical use in type 2 diabetes. Diabetologia 60:1586–1593. https://doi.org/10.1007/s00125-017-4336-x
Scheurer M, Michel A, Brauch HJ et al (2012) Occurrence and fate of the antidiabetic drug metformin and its metabolite guanylurea in the environment and during drinking water treatment. Water Res 46:4790–4802. https://doi.org/10.1016/j.watres.2012.06.019
Scialdone O, Galia A, Guarisco C et al (2008) Electrochemical incineration of oxalic acid at boron doped diamond anodes: role of operative parameters. Electrochim Acta 53:2095–2108. https://doi.org/10.1016/j.electacta.2007.09.007
Tisler S, Zwiener C (2018) Formation and occurrence of transformation products of metformin in wastewater and surface water. Sci Total Environ 628–629:1121–1129. https://doi.org/10.1016/j.scitotenv.2018.02.105
Tong AZ, Ghoshdastidar AJ, Fox S (2015) The presence of the top prescribed pharmaceuticals in treated sewage effluents and receiving waters in southwest Nova Scotia, Canada. Environ Sci Pollut Res 22:689–700. https://doi.org/10.1007/s11356-014-3400-z
Trautwein C, Kümmerer K (2011) Incomplete aerobic degradation of the antidiabetic drug Metformin and identification of the bacterial dead-end transformation product Guanylurea. Chemosphere 85:765–773. https://doi.org/10.1016/j.chemosphere.2011.06.057
Vasilie S, Manea F, Baciu A, Pop A (2018) Dual use of boron-doped diamond electrode in antibiotics-containing water treatment and process control. Process Saf Environ Prot 117:446–453. https://doi.org/10.1016/j.psep.2018.05.024
Wang X, Sun C, Gao S et al (2001) Validation of germination rate and root elongation as indicator to assess phytotoxicity with Cucumis sativus. Chemosphere 44:1711–1721. https://doi.org/10.1016/S0045-6535(00)00520-8
WHO (2016) Global report on diabetes. ISBN 978:6–86
Yan JH, Xiao Y, Tan DQ et al (2019) Wastewater analysis reveals spatial pattern in consumption of anti-diabetes drug metformin

in China. Chemosphere 222:688–695. https://doi.org/10.1016/j.chemosphere.2019.01.151

Yang PK, Hsu CY, Chen MJ et al (2018) The efficacy of 24-month metformin for improving menses, hormones, and metabolic profiles in polycystic ovary syndrome. J Clin Endocrinol Metab 103:890–899. https://doi.org/10.1210/jc.2017-01739

Zayneb C, Lamia K, Olfa E et al (2015) Morphological, physiological and biochemical impact of ink industry effluent on germination of Maize (Zea mays), Barley (Hordeum vulgare) and Sorghum (*Sorghum bicolor*). Bull Environ Contam Toxicol 95:687–693. https://doi.org/10.1007/s00128-015-1600-y

Zhang Z, Li F, Tian Y et al (2020) Metformin enhances the antitumor activity of CD8 + T lymphocytes via the AMPK–miR-107–eomes–PD-1 pathway. J Immunol 204:2575–2588. https://doi.org/10.4049/jimmunol.1901213

Zhu S, Liu Y, guo, Liu S bo, et al (2017) Adsorption of emerging contaminant metformin using graphene oxide. Chemosphere 179:20–28. https://doi.org/10.1016/j.chemosphere.2017.03.071